

# High-Order Integration of Fatigue Crack Growth Using Surrogate Model

Matthew J. Pais\*, Felipe A. C. Viana†, and Nam-Ho Kim‡  
*University of Florida, Gainesville, FL 32611*

Modeling fatigue crack growth is a challenging computational fracture mechanics problem because the crack growth rate can only be evaluated at the current crack size. The forward Euler method has been a common choice in integrating fatigue crack growth, whose accuracy can only be guaranteed with a very small size of increment. This hinders failure investigation of systems with complex geometry, which would require expensive finite element simulations. Higher-order integration methods, such as the midpoint method, might allow larger increment size but require additional evaluation of crack growth rate at crack sizes larger than the current one. In arbitrary geometry, this is not an easy task because the direction of crack growth is unknown in advance, and additional simulations are often prohibitive. In this paper, two surrogate models are generated for the prior crack growth direction and stress intensity factor data and are used to predict the crack growth rate at future locations without the need for additional finite element simulations. The step size for the numerical integration is chosen based on the prior accuracy of the extrapolated data for the crack growth direction and stress intensity factor. Several examples were tested in which crack growth follows linear and curved paths under a range of boundary conditions leading to different relationships between stress intensity factor and crack size. Results showed that a large increase in the allowable step size may be used with increased accuracy over the Euler method without the need for additional simulations.

## Nomenclature

$a$	=	characteristic crack length
$a_i$	=	initial crack length
$a_N$	=	crack length at cycle $N$
$C$	=	Paris Law constant
$K_I$	=	mode I stress intensity factor
$K_{II}$	=	mode II stress intensity factor
$m$	=	Paris Law exponent
$N$	=	number of elapsed cycles
$\Delta a$	=	increment of crack growth
$\Delta K$	=	stress intensity factor range
$\Delta K_{eq}$	=	equivalent stress intensity factor range
$\Delta N$	=	increment of elapsed number of cycles
$\theta_c$	=	crack growth direction

---

\* Graduate Research Assistant, Department of Mechanical and Aerospace Engineering, PO Box 116250, University of Florida, Gainesville, FL 32611-6250, mpais@ufl.edu, Student Member.

† Graduate Research Assistant, Department of Mechanical and Aerospace Engineering, PO Box 116250, University of Florida, Gainesville, FL 32611-6250, fchegury@ufl.edu, Student Member.

‡ Associate Professor, Department of Mechanical and Aerospace Engineering, PO Box 116250, University of Florida, Gainesville, FL 32611-6250, nkim@ufl.edu, AIAA Member.

## I. Introduction

MODELING fatigue crack growth is a challenging problem in computational fracture mechanics. The large number of loading cycles ( $10^3$ - $10^8$ ) which causes eventual failure requires methods to reduce the number of simulations needed to model fatigue crack growth. The two traditional approaches to numerically integrate the crack growth are (a) to assume a fixed increment of crack growth at each iteration<sup>1</sup> or (b) to assume a constant number of cycles at each iteration<sup>2</sup>. Initially the former uses a large number of cycles at each iteration because the rate of crack growth is slow, and gradually decreases the number of cycles as the rate increases. Evaluating fatigue crack growth directly in terms of the number of elapsed cycles has been challenging as the crack grows rapidly as it approaches the critical crack size, which can lead to numerical instability<sup>3</sup>. A similar problem occurs for the case of a constant number of cycles at each iteration.

Fatigue crack growth is commonly governed by an ordinary differential equation of the general form<sup>4</sup>

$$\frac{da}{dN} = f(\Delta K, R) \quad (1)$$

where  $\Delta K$  is the stress intensity factor range and  $R$  is the stress ratio. Note that the number of cycles,  $N$ , is considered a continuous number in the above equation. Although  $\Delta K$  depends on the characteristic crack length  $a$ , there is no analytical equation available except for simple cases. Thus, numerical integrations are commonly employed to solve the differential equation. In addition, the evaluation of  $f(\Delta K, R)$  requires numerical analysis, such as finite element analysis. With given conditions, the solution of the ordinary differential equation given by Eq. (1) generally cannot be obtained using an exact solution to the governing differential equation as the expression of  $f(\Delta K, R)$  is not known *a priori*. Due to the lack of available knowledge about the function  $f(\Delta K, R)$ , it is not trivial to apply different integration methods because it may not be possible to evaluate  $f(\Delta K, R)$  at any point.

Challenges associated with remeshing<sup>5</sup> about the crack tip as growth occurs in the classical finite element approaches can be avoided through the use of the extended finite element method<sup>1</sup> (XFEM). For an arbitrary crack and geometry a numerical method such as the XFEM can be used to find the values of  $\Delta K$  at the current iteration of crack growth. Through a series of XFEM simulations, it is possible to generate data points and approximate the right-hand side of Eq. (1). Until the completion of the finite element simulations,  $f(\Delta K, R)$  is an unknown function. The relationship given in Eq. (1) is typically a monotonically increasing function for the relationships between  $\Delta K$ ,  $a$ , and  $N$  as shown in Figure 1, whose exact shape is a function of geometric properties, loading conditions, and material properties.

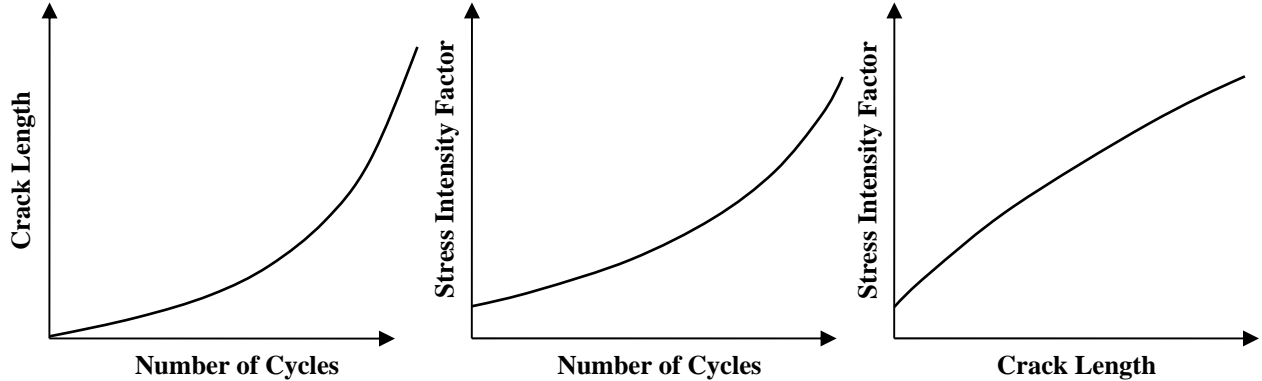


Figure 1. The relationships between  $\Delta K$ ,  $a$ , and  $N$ .

The common practice is to use the forward Euler approximation to the fatigue crack growth law at each iteration to find the magnitude and direction of crack growth. The choice is not because of its capability, but because of convenience. This method requires evaluating  $f(\Delta K, R)$  at the current crack geometry, while other methods need it at the future crack geometry. However, this method requires a small step size to maintain stability and accuracy of the solution. This limits the step size of crack growth increment  $\Delta a$  or elapsed cycle increment  $\Delta N$  for the

forward Euler approximation to be accurate. Notice that due to the monotonic relationships as shown in Figure 1, the forward Euler method will always under predict  $a$  and  $\Delta K$  from  $N$  and over predict  $\Delta K$  from  $a$ . Thus, as soon as the approximation under or over predicts the quantity being approximated, it will continue to under or over predict the quantity with increasing error as future iterations occur. Higher-order approximations such as the midpoint method could be used to address this issue, but each method requires additional simulations for the slope evaluations needed for these higher order approximations.

Instead, surrogate models can be used to alleviate the cost associated with such higher-order integrators. Surrogate modeling (also known as metamodeling or response surface approximation) consists of analyzing a number of designs, fitting a surrogate, then replacing the costly simulations by the surrogate model<sup>6-9</sup>. The basic idea is to use the history of stress intensity factors up to the current cycle to build a surrogate model and predict the stress intensity factor at different crack sizes or different cycles. New data points can be added to the original set as the simulation evolves and more data points are available for the surrogate model. Even though there is a large variety of techniques in the literature (e.g., polynomial response surface<sup>10</sup>, kriging<sup>11-13</sup>, radial basis neural networks<sup>14</sup>, and support vector regression<sup>15</sup>), in this work kriging was chosen because of its popularity in the surrogate modeling community and because of features such as interpolation.

Here two cases are considered. First, the approach of fitting surrogate models to the stress intensity factor and crack growth direction history is tested based on a fixed increment of crack growth  $\Delta a$  or a fixed number of elapsed cycles  $\Delta N$  per iteration. When  $\Delta a$  is fixed, the relationship between  $\Delta K$  and  $\Delta a$  is fitted using a kriging surrogate. This surrogate is then used to approximate the corresponding  $\Delta N$  for a given  $\Delta a$  such that the cyclic crack growth history can be obtained. Correspondingly, when  $\Delta N$  is fixed, the relationship between  $\Delta K$  and  $\Delta N$  is fitted using a kriging surrogate. This surrogate is then used to extrapolate forward in time so that a higher order approximation to the chosen fatigue crack growth law can be used to find the corresponding  $\Delta a$ . Second, a variable step size algorithm is introduced for the automatic generation of a step size  $\Delta N$  based on the accuracy in the surrogate extrapolation of  $\Delta K$  and the crack growth direction.

Two examples are presented with known relationships between  $\Delta K$  and  $a$ . A center crack in an infinite plate under uniaxial tension is considered first. For a fixed  $\Delta a$ , the Euler and midpoint approximations are compared to the case of the kriging assisted midpoint approximation. For a fixed  $\Delta N$ , the Euler and midpoint approximations are compared to the case of kriging assisted midpoint approximation. As the relationship between  $\Delta K$  and  $a$  is known, the variable step size algorithm is applied. Finally, the XFEM<sup>1</sup> is used to model mixed-mode crack growth for an inclined center crack in a finite plate and an edge crack in a finite plate with a hole. The results show that a larger step size can be used with increased accuracy with the use of kriging assisted approximations for the solution of fatigue crack growth laws.

## II. Methods of Solving an Ordinary Differential Equation

For an arbitrary differential equation of the form  $y'(x) = f(x, y(x))$  the goal is to predict the value of  $y_{n+1}$  while the current data is available up to  $y_n$ . The simplest numerical method available which is applicable to the current crack growth problem is the explicit forward Euler method<sup>16</sup> given as

$$y_{n+1} = y_n + hf(x_n, y_n) \quad (2)$$

where  $h$  is the step size from  $x_n$  to  $x_{n+1}$ . Note that  $f(x_n, y_n)$  is the slope of  $y(x)$  at  $x_n$ ; therefore a linear approximation is being made from  $x_n$  to  $x_{n+1}$  using the slope at the  $x_n$ . This method has been popular in engineering applications because it only requires evaluating the slope at the current step, which often required expensive computational simulation. For example, in the case of crack growth simulation,  $f(x_n, y_n)$  corresponds to calculating the stress intensity factor with given crack size  $y_n$ . Therefore, evaluating  $f(x_n, y_n)$  requires a finite element modeling with the current geometry of the crack. If a different method, such as the backward Euler method, is used, then  $f(x_{n+1}, y_{n+1})$  is required, which is the stress intensity factor corresponding to the unknown crack size

$y_{n+1}$ . Therefore, there exists a fundamental difficulty to use a numerical integration method other than the forward Euler method.

Although the forward Euler method can resolve the issue related to evaluating the slope at unknown crack sizes, it has a drawback in slow convergence; the accuracy of the method is proportional to the step size,  $h$ . In crack growth analysis, the step size represents the number of fatigue loading cycles between two evaluation points. Since cracks grow slowly throughout the lifecycle of a product, a small step size means tens of thousands of simulations. Therefore, it is highly desired to use a numerical integration method that allows a larger step size, while maintaining accuracy.

There are numerous numerical methods that allow larger step sizes for integration, but the midpoint integration method is used as a demonstration tool in this paper. The midpoint method<sup>16</sup> generally provides a better accuracy than the forward Euler method as it takes the slope at the midpoint between the current and future data points  $x_{n+1/2}$  and uses that value to approximate the interval from  $x_n$  to  $x_{n+1}$  such that the approximation is given as

$$y_{n+1} = y_n + hf \left( x_n + \frac{h}{2}, y_n + \frac{h}{2} f(x_n, y_n) \right). \quad (3)$$

The accuracy of the method is proportional to  $h^2$ ; therefore, it allows a larger step size for the same accuracy with the forward Euler method. However, this method requires evaluating the slope at the advanced half step. In practice, this is not an easy task because the crack size at the advanced step is unknown; it is a part of the solution. In addition, in a complex system, the direction of crack growth may not be constant, and thus, it would be difficult to build a numerical model to calculate the slope at the advanced step. The midpoint approach is taken for both the magnitude and direction of crack growth in the proposed algorithm.

### III. Fatigue Crack Growth

#### A. Fatigue Crack Growth Model

There are many fatigue crack growth models available in the literature<sup>4</sup>. One of the first attempts to create a model to represent fatigue crack growth was that of Paris<sup>17</sup>. The Paris model is well known and takes the form

$$\frac{da}{dN} = C (\Delta K)^m \quad (4)$$

where  $da/dN$  is the crack growth rate,  $C$  and  $m$  are model parameters, and  $\Delta K$  is the range of Mode I stress intensity factor. An analytical solution of Eq. (4) is available for the simplest case that is an infinite plate under Mode I configuration. Other cases require numerical integration in order to calculate the crack growth as a function of fatigue loading cycle  $N$ .

The solution of Eq. (4) with respect to modeling crack growth with finite element simulations has taken two main approaches. First, a fixed crack growth increment  $\Delta a$  can be considered. Once the simulations have completed, the relation between  $\Delta a$  and  $\Delta K$  can be used to find the corresponding  $\Delta N$  for each iteration. For a fixed increment of elapsed cycles  $\Delta N$  can be considered. Here, at each iteration  $\Delta a$  is approximated based on the selected  $\Delta N$  and the iteration dependent  $\Delta K$ . Either method is capable of yielding an accurate representation of the fatigue crack growth behavior for a given structure should an appropriate step size of  $\Delta a$  or  $\Delta N$  be chosen. Second, an automated variable step size algorithm has been introduced to distribute the simulations in a controlled manner with the goal of reducing the number of simulations needed without a loss in accuracy.

When there are nonzero Mode II stress intensity factors present, it is necessary to consider an equivalent stress intensity factor range as well as a direction of crack growth. There are many ways to find an equivalent stress intensity factor range<sup>18-20</sup>. Here the method proposed by Tanaka<sup>19</sup> is used:

$$\Delta K_{eq} = \sqrt[4]{\Delta K_I^4 + 8\Delta K_{II}^4} \quad (5)$$

where  $\Delta K_I$  and  $\Delta K_{II}$  are the ranges of mode I and II stress intensity factors. The direction of crack growth is also assumed here to be the direction which will maximize the opening Mode I stress intensity factor. This angle

for any combination of mixed mode loading consisting of Mode I and Mode II is given by the maximum circumferential stress criterion<sup>21</sup> as

$$\theta = 2 \arctan \frac{1}{4} \left( \frac{K_I}{K_{II}} - \text{sign}(K_{II}) \sqrt{\left( \frac{K_I}{K_{II}} \right)^2 + 8} \right). \quad (6)$$

Note, that this is in essence an Euler approximation to the crack growth direction as it only considers the stress intensity factors at the  $i$ th data point. As mentioned before, when the geometry of the plate is finite and the applied load generates mixed mode, it is not easy to calculate  $\Delta K_{i+1/2}$  and  $\Delta K_{i+1}$ . This requires building a finite element model with crack size at  $i + 1 / 2$  and  $i + 1$  iterations. However, without calculating crack sizes and directions at the advanced iterations, it is not possible to calculate stress intensity factors. Thus, except for the forward Euler method, some kind of approximation should be adopted to estimate the range of stress intensity factors at the advanced. In the following section, a surrogate modeling technique will be presented to approximate the range of stress intensity factor as well as the crack growth direction allowing for a midpoint approximation to be applied to both the magnitude and direction of crack growth for a given crack through the use of surrogate modeling.

## B. Numerical Integration of the Fatigue Crack Growth Model

### 1. Forward Euler Method

The simplest approach to integrating the Paris model for fatigue crack growth is the use of the forward Euler method. Here the stress intensity factor range at the current iteration is the only information needed to find the increment of growth between the current and future iterations. The growth increment may be calculated as

$$\Delta a_i = \Delta N \left[ C (\Delta K_i)^m \right] \quad (7)$$

where  $i$  is the current increment. The corresponding number of elapsed cycles can be approximated as

$$\Delta N_i = \frac{\Delta a}{C (\Delta K_i)^m} \quad (8)$$

for a fixed increment of crack growth. As the forward Euler method only uses the slope at the current point and linearly interpolates to the next crack size it can lead to large inaccuracies for relatively small crack growth increments. Although the physical meaning of  $\Delta N$  is the number of elapsed cycles, in this model it is treated as a continuous variable as crack growth occurs over tens of thousands of cycles. Choosing a larger  $\Delta N$  results in needing fewer finite element simulations while sacrificing accuracy.

### 2. Midpoint Integration Method

The next approach to integrating the Paris model is the use of the midpoint method where the growth increment is calculated as

$$\Delta a_i = \Delta N \left[ C (\Delta K_{i+1/2})^m \right] \quad (9)$$

where  $i + 1 / 2$  is the midpoint between the current and next increment. Similarly,  $\Delta N_i$  is given as

$$\Delta N_i = \frac{\Delta a}{C (\Delta K_{i+1/2})^m}. \quad (10)$$

Here the slope at the midpoint of the current cycle is used to extrapolate ahead to  $i + 1$ . This leads to a better approximation of the crack size at the next increment as a more accurate approximation of the slope over the entire interval of the chosen growth increment is used. This method, however, requires an additional function evaluation at  $i + 1 / 2$  for each iteration being considered, effectively doubling the number of function evaluations needed for the given simulation.

## C. Variable Step Size Algorithm

Two algorithms are provided for the use of surrogate models, the first model is based on the accuracy of the extrapolation of the surrogate during the previous iteration of crack growth. This algorithm should be useful for any surrogate model. Other surrogates may or may not have an easily defined uncertainty structure. For the case

of adjusting the step size based on the prior accuracy, the step size for the  $i+1^{\text{th}}$  iteration can be found from the  $i^{\text{th}}$  iteration as

$$\Delta N_{i+1} = \Delta N_i \min \left[ \left( \frac{a_k}{\left| 1 - \frac{\Delta K_{i+1}^{SUR}}{\Delta K_{i+1}^{NUM}} \right|} \right)^{\alpha_k}, \left( \frac{a_t}{\left| 1 - \frac{\theta_{i+1}^{SUR}}{\theta_{i+1}^{NUM}} \right|} \right)^{\alpha_t} \right] \quad (11)$$

where  $\Delta N_i$  is the current step size,  $a$  is the allowable percent difference between the surrogate extrapolation and XFEM values at  $i+1$ ,  $\alpha$  is an exponent which determines how quickly the step size changes, and  $\Delta K_{i+1}$  and  $\theta_{i+1}$  are evaluated based on  $i+1$  for the current iteration using either a numerical (e.g. XFEM) or surrogate (e.g. kriging) model. The step size is scaled based on the accuracy of the predicted value. For the case where either  $\Delta K_{i+1}^{SUR} = \Delta K_{i+1}^{NUM}$  or  $\theta_{i+1}^{SUR} = \theta_{i+1}^{NUM}$ , then  $\Delta N_{i+1} = 2\Delta N_i$ .

#### IV. Use of Surrogate Model in Integration

The limitation on the types of methods which can be used in the direct integration of a fatigue model come from the need to evaluate the stress intensity factor at some future crack tip position. Because this crack position is unknown, it is unclear how to apply a numerical method to address this challenge. The idea presented here is to use a surrogate model to fit the available stress intensity factor history. The surrogate model can then be used to extrapolate ahead of the current crack position to get an estimate of the stress intensity factor which can then be used for a higher-order integration method. Visually, this is shown in Figure 2 where the filled circles represent current or past numerical data points, the empty circle represents the data point to be solved for currently, and the empty square represents the surrogate extrapolation. The solid line denotes the surrogate model for the given data points, while the dot-dashed and dashed lines represent the approximation based on Euler and midpoint approximations of the solution.

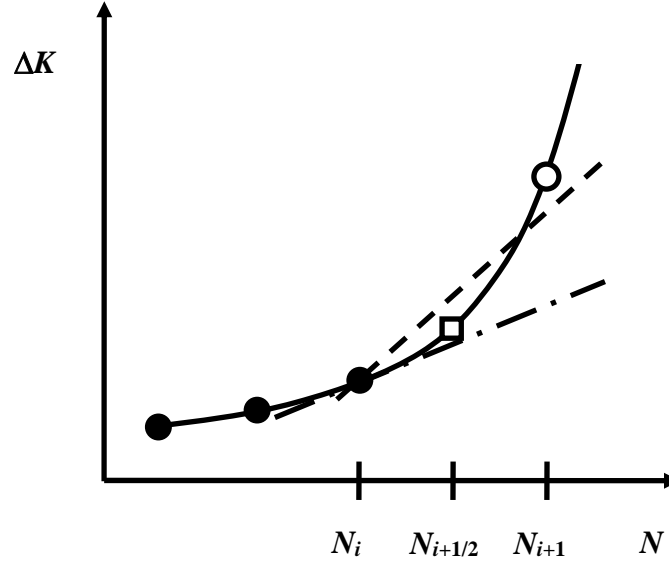


Figure 2. The use of a surrogate model to extrapolate ahead of the current data point, allowing higher-order integration of the governing fatigue crack growth model.

In this paper, results are presented for the kriging surrogate. Kriging was used here as the winner of an initial round robin tournament involving a variety of kriging, polynomial, radial basis neural network, and support vector regression surrogates. The details of kriging are given in Appendix A, but the methods presented here should be applicable to any surrogate model which provides sufficient extrapolation accuracy.

For problems with mixed mode loading, two kriging surrogates are used. First, a kriging surrogate is used to approximate the response of  $\Delta K$  as a function of either the crack length  $a$  or the number of elapsed cycles  $N$ . The kriging approximation is then used for a higher order approximation to Paris Law, such as the midpoint method

given by Eq. (9). For the case of a fixed  $\Delta a$ ,  $\Delta N$  is calculated *a posteriori* to the simulations using interpolation between data points. Equally spaced data points between  $a_i$  and the final crack length are fitted using kriging. This surrogate is then used to interpolate between data points and evaluate the corresponding  $\Delta N$  for each  $\Delta a$ . For a fixed  $\Delta N$ , kriging is used to fit the data up to the current cycle and extrapolate approximate values of  $\Delta K$  for the use of the midpoint method. Second, a kriging surrogate is used to approximate the angle of crack growth  $\theta$ . Four initial data points are provided before the use of kriging. To get the three additional data points, the forward Euler method can be used as its accuracy is sufficient away from the critical crack length. Two algorithms are provided for the selection of a variable step size for direct fatigue evaluation. A general form is introduced based on the agreement between the stress intensity factor and crack growth direction values for the surrogate extrapolation and the theoretical or XFEM values, as in Eq. (11).

## V. Results

First a center crack in an infinite plate under uniaxial tension is considered. This case is convenient as it has a closed form solution for the crack size and stress intensity factor as a function of applied stress, loading cycle, and material properties. This allows for an estimate of the amount of error that can be expected by the use of kriging to provide data points instead of performing a simulation. The effect on the choice of a fixed  $\Delta a$  or  $\Delta N$  is considered for the theoretical model of a center crack in an infinite plate to show the validity of the approach. The presented variable step size algorithm is also used for each example problem. Results are presented for each case as the final approximate value normalized by the exact final value of crack size or cycle number. A value of one denotes perfect agreement with the exact solution.

The chosen geometry for all problems is a flat, square plate under uniaxial tension of 78.6 MPa. The plate is considered to be infinite in problem A, the plate width for problem B was 0.2 m, and the plate width for problem C was 2 m. The tested materials and the corresponding material properties are aluminum 2024 at stress ratios of 0.1 ( $C = 1.60 \cdot 10^{-11}$ ,  $m = 3.59$ ) and 0.5 ( $C = 3.15 \cdot 10^{-11}$ ,  $m = 3.59$ ) as well as austenitic ( $C = 1.36 \cdot 10^{-10}$ ,  $m = 2.25$ ) and martensitic ( $C = 5.60 \cdot 10^{-12}$ ,  $m = 3.25$ ) steel<sup>23</sup>. Data is simulated until the point at which  $\Delta K_{eq}$  has exceeded  $K_{IC}$  (30 MPa $\sqrt{m}$  for aluminum and 50 MPa $\sqrt{m}$  for steel). The results are presented for each case as a function of the ratio between the exact final and predicted final crack size or cycle number such that a value of one denotes the exact solution.

A series of XFEM simulations were performed to evaluate  $\Delta K^{NUM}$  as a function of the crack size  $a$ . In addition, the angle of crack growth given in terms of the global coordinate system  $\theta^{NUM}$  was evaluated as a function of crack size. A brief summary of the XFEM is given in Appendix B. Once these easily evaluated functions were available, the crack growth was simulated such that:

1. For iteration  $i$ , fit surrogate for history of  $\Delta K^{NUM}$  and  $\theta^{NUM}$ , evaluate  $\Delta K^{SUR}$  and  $\theta^{SUR}$  at  $i+1/2$  and  $i+1$ .
2. Calculate the crack growth increment  $\Delta a$  from  $\Delta a = \Delta N_i C \left( \Delta K_{i+1/2}^{SUR} \right)^m$ .
3. Calculate the crack growth increments in the x and y-directions from  $\Delta x = \Delta a \cos\left(\theta_{i+1/2}^{SUR}\right)$  and  $\Delta y = \Delta a \sin\left(\theta_{i+1/2}^{SUR}\right)$ .
4. Update the crack tip location based on  $\Delta x$  and  $\Delta y$  followed by evaluating  $\Delta K_{i+1}^{NUM}$  and  $\theta_{i+1}^{NUM}$ .
5. Find the next step size based on the criteria in Eq. (11), repeat for next iteration.

### A. Center Crack in an Infinite Plate under Tension

First, a center crack in an infinite plate with initial crack length of 10 mm is considered. For the case of a center crack in an infinite plate under uniaxial tension, the Mode I stress intensity factor<sup>24</sup> is

$$K_I = \sigma \sqrt{\pi a} \quad (12)$$

where  $\sigma$  is the applied stress, and  $a$  is the half crack length. By substituting Eq. (12) into Eq. (4) for Paris Law and rearranging terms, the number of cycles for a crack to grow can be calculated using the following integration:

$$N = \int_{a_i}^{a_N} \frac{da}{C(\sigma\sqrt{\pi a})^m} = \left[ \frac{a_N^{\frac{2-m}{2}} - a_i^{\frac{2-m}{2}}}{C\left(\frac{2-m}{2}\right)(\sigma\sqrt{\pi})^m} \right] \quad (13)$$

where  $a_i$  is the initial crack size. In another way, the crack size  $a_N$  after  $N$  cycles can be calculated by

$$a_N = \left[ NC\left(1 - \frac{m}{2}\right)(\sigma\sqrt{\pi})^m + a_i^{\frac{2-m}{2}} \right]^{\frac{2}{2-m}}. \quad (14)$$

This allows for the midpoint method to be applied as  $a_N$  and  $K_I$  can be directly evaluated and used in the integration of Paris model at any cycle number.

An aluminum 2024 plate with a stress ratio of 0.5 is chosen to validate the use of kriging extrapolation for the integration of the fatigue crack growth model. The critical stress intensity factor is reached for a crack size of 50 mm given an initial crack size of 10 mm in about 22,300 cycles. For a fixed  $\Delta a$ , the results are given in Table 1. Recall that the common  $\Delta a$  used in the literature<sup>1</sup> is  $a_i/10$ . The second and third columns are the accuracy of numerical integration with Euler and midpoint methods, respectively, when exact stress intensity factor is used. The last column is the accuracy of midpoint method when the kriging surrogate is used in approximating the stress intensity factor. For that crack growth increment, the Euler approximation has over 5 percent error. Through the use of the midpoint approximation, the error is reduced to less than 1 percent. Larger crack growth increments for the Euler method lead to very large errors, which can be drastically reduced through the use of a higher-order approximation. Note also that the use of kriging to fit data and to provide estimates for the necessary function evaluations for the higher-order approximations results in no loss of accuracy.

Table 1. Accuracy of integration for chosen  $\Delta a$  for a center crack in an infinite plate of Al 2024 (R = 0.5).

$\Delta a$	Euler	Midpoint	$N_{\text{approx}}/N_{\text{exact}}$ Kriging Extrapolation and Midpoint
$a_i/160$	1.0033	1.0000	1.0000
$a_i/80$	1.0065	1.0000	0.9999
$a_i/40$	1.0131	0.9999	0.9999
$a_i/20$	1.0264	0.9998	0.9998
$a_i/10$	1.0536	0.9992	0.9992
$a_i/5$	1.1105	0.9968	0.9968
$a_i/2$	1.2992	0.9810	0.9811
$a_i$	1.6635	0.9348	0.9436

For a fixed  $\Delta N$ , the results are given in Table 2. The first observation from Table 2 is that the accuracy of Euler approximations is much more sensitive to changes in fixed  $\Delta N$  when compared to a fixed  $\Delta a$ . However, the midpoint approximations are largely insensitive to the chosen crack growth increment. As before, the kriging assisted midpoint approximation is very accurate and comparable to using the exact formula.

Table 2. Accuracy of integration for chosen  $\Delta N$  for a center crack in an infinite plate of Al 2024 (R = 0.5).

$\Delta N$	Euler	Midpoint <sup>§</sup>	$a_{\text{approx}}/a_{\text{exact}}$ Kriging Extrapolation and Midpoint
1	0.9998	1.0001	1.0000
25	0.9950	1.0001	0.9999
50	0.9901	1.0001	0.9998
100	0.9806	1.0001	0.9993
500	0.9184	0.9998	0.9987
1000	0.8562	0.9988	0.9953

<sup>§</sup> For a center crack in an infinite plate, the midpoint method can be used through Eq. (14). For an arbitrary geometry the midpoint method cannot be used. It is used here to assess the error introduced by the kriging extrapolation.



To assess the applicability of the variable step size algorithm to a range of fatigue problems four different aerospace materials were chosen along with initial crack sizes of either 1 or 10 mm and grown to failure at 50 mm. As with the fixed step size approach, three data points are found using the forward Euler approach with  $\Delta N = 1$  before the variable step size algorithm begins. The values of  $a_k$  and  $a_t$  in Eq. (11) were found to be 0.001, while  $\alpha_t$  and  $\alpha_k$  were defined to be 0.1 based on a parameter study. The results for the materials and crack sizes is given in Table 3

Table 3. Effect of material and initial crack size on estimated cycles to failure.

Material	$a_i$ [mm]	$N_{fail}^{euler}, I_{\Delta N=1}^{euler}$	$I_{var}^{KRG}$	$N_{fail}^{KRG}$	$N_{fail}^{KRG} / N_{fail}^{euler}$	$I_{var}^{KRG} / I_{var}^{euler}$
2024, R = 0.1	1	364,676	49	369,169	1.0123	1.3E-4
2024, R = 0.1	10	43,237	38	43,437	1.0046	8.8E-4
2024, R = 0.5	1	185,232	48	188,126	1.0156	2.6E-4
2024, R = 0.5	10	21,962	38	22,053	1.0041	1.7E-3
Austenitic	1	951,320	46	957,139	1.0061	4.8E-5
Austenitic	10	428,539	46	429,546	1.0023	1.1E-4
Martensitic	1	2,193,024	75	2,225,481	1.0148	3.4E-5
Martensitic	10	435,647	47	438,664	1.0069	1.1E-4

Note that the number of iterations for the Euler method is the same as  $N_{fail}^{euler}$ . It can be noted from the above table that the number of iterations that the algorithm uses to model the crack growth to failure is generally independent of the number of cycles to failure. The general trend of the variable step size algorithm is that initially there are smaller steps, then the step size increases. As the crack approaches the critical crack size, the step size decreases. This trend is shown in section C of the results in Figure 4 and Figure 5.

## B. Edge Crack in a Finite Plate under Tension

For the case of an edge crack in a finite plate under uniaxial tension the Mode I stress intensity factor<sup>24</sup> is

$$K_I = \left[ 1.12 - 0.281 \frac{a}{W} + 10.55 \left( \frac{a}{W} \right)^2 - 21.72 \left( \frac{a}{W} \right)^3 + 30.39 \left( \frac{a}{W} \right)^4 \right] \sigma \sqrt{\pi a} \quad (15)$$

where  $a$  is the crack length and  $W$  is the plate width. As there is no analytical expression for  $a_N$ , the crack length after 10,700 cycles was found to be 30 mm using the forward Euler method where the step size was reduced until convergence in crack size at 10,700 cycles was achieved.

For a fixed step size, aluminum 2024 with a stress ratio of 0.5 is chosen to validate the use of kriging extrapolation for the integration of the fatigue crack growth model with a constant step size. The critical stress intensity factor is reached for a crack size of 30 mm given an initial crack size of 10 mm in about 11,000 cycles. For a fixed  $\Delta a$ , the results are given in Table 4. Here for a fixed crack growth increment of  $a_i/10$  the corresponding Euler approximation is off by 7 percent, while the midpoint approximation yields less than 1 percent error.

Table 4. Accuracy of integration methods for chosen constant  $\Delta a$  for an edge crack in a finite plate.

Constant $\Delta a$	Euler	Midpoint	$N_{approx}/N_{exact}$ Kriging Extrapolation and Midpoint
$a_i/160$	1.0000	0.9957	0.9957
$a_i/80$	1.0043	0.9957	0.9957
$a_i/40$	1.0129	0.9957	0.9957
$a_i/20$	1.0303	0.9954	0.9954
$a_i/10$	1.0661	0.9946	0.9946
$a_i/5$	1.1409	0.9912	0.9912
$a_i/2$	1.3906	0.9693	0.9729
$a_i$	1.8759	0.9052	0.9436

For a fixed elapsed number of cycles in each simulation, the exact results for the midpoint method are not available as there is no explicit value for  $a_N$ . From Table 5 it is apparent that once again, the kriging assisted

midpoint method allows for larger step sized compared to the forward Euler method. In this case, for a step size of 100, the errors for the Euler and kriging assisted midpoint methods are 3.5 and 0.2 percent. The similar trend of the kriging assisted midpoint method being less accurate for larger  $\Delta N$  continues, and that approximation is still better than Euler alone. The increased errors in the approximation compared to the case of a center crack in an infinite plate can most likely be explained by the increased nonlinearity caused by the edge and finite effects present in this geometry.

Table 5. Accuracy of integration methods for chosen constant  $\Delta N$  for an edge crack in a finite plate.

Constant $\Delta N$	Euler	Midpoint**	$a_{\text{approx}}/a_{\text{exact}}$ Kriging Extrapolation and Midpoint
1	1.0000	N/A	1.0000
25	0.9935	N/A	0.9999
50	0.9869	N/A	0.9990
100	0.9745	N/A	0.9987
500	0.9468	N/A	0.9950
1000	0.8707	N/A	0.9778

The variable step size algorithm is again tested with a range of fatigue problems. Four different aerospace materials were chosen along with initial crack sizes of either 1 or 10 mm and grown to failure at 50 mm. As with the fixed step size approach, three data points are found using the forward Euler approach with  $\Delta N = 1$  before the variable step size algorithm begins. The previously determined values for  $a_k$  and  $a_t$  were found to be 0.001, while  $\alpha_t$  and  $\alpha_k$  were defined to be 0.1 based on a parameter study. The results for the materials and crack sizes are given in Table 6. Note that there is an increased error for this case can be attributed to the  $a/W$  relationship present in Eq. (15).

Table 6. Effect of material and initial crack size on estimated cycles to failure.

Material	$a_i$ [mm]	$N_{\text{fail}}^{\text{euler}}, I_{\Delta N=1}^{\text{euler}}$	$I_{\text{var}}^{\text{KRG}}$	$N_{\text{fail}}^{\text{KRG}}$	$N_{\text{fail}}^{\text{KRG}} / N_{\text{fail}}^{\text{euler}}$	$I_{\text{var}}^{\text{KRG}} / I_{\text{var}}^{\text{euler}}$
2024, R = 0.1	1	235,374	42	240,401	1.0214	
2024, R = 0.1	10	20,701	38	21,473	1.0373	
2024, R = 0.5	1	119,557	44	122,705	1.0263	
2024, R = 0.5	10	10,516	38	10,799	1.0269	
Austenitic	1	594,634	49	601,308	1.0112	
Austenitic	10	189,225	41	193,493	1.0226	
Martensitic	1	1,415,883	46	1,459,668	1.0309	
Martensitic	10	196,924	41	200,215	1.0167	

### C. Inclined Center Crack in a Finite Plate Under Uniaxial Tension

The first test problem which also considers the effect of crack growth direction is that of an inclined center crack in a finite plate subjected to uniaxial tension in the y-direction as shown in Figure 3. The plate was chosen to be a 2 m x 2 m plate with an initial half crack size of 0.187 m. The crack was grown by XFEM to a final half crack size of 0.6 m. The values of the constants in the variable step size algorithm were retained from the previous sections.

\*\* Due to the inability to exactly integrate Paris model with the stress intensity factor of Eq. (15), it is not possible to use the midpoint method for this problem.

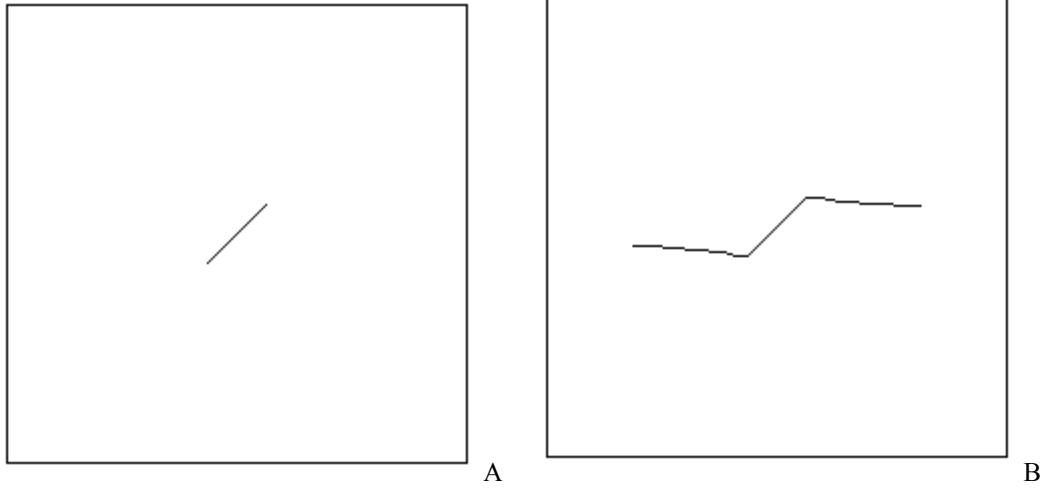


Figure 3. Initial (A) and final (B) crack geometries for an inclined center crack in a finite plate under uniaxial tension.

For the variable step size algorithm, different applied stresses were considered in order to make the Euler approximation feasible. The comparison of the number of cycles to failure and the final crack position for the Euler with constant  $\Delta N = 1$  to the variable step size algorithm for the functions for  $\Delta K$  and  $\theta$  is presented in Table 7. Note that the cycle number corresponding to failure in each case is in excellent agreement with the XFEM solution, but with substantially less iterations needed for the solution. The step size trends and the errors as a function of cycle number for both stress ratios for aluminum 2024 are given in Figure 4 and Figure 5.

Table 7. Sensitivity study of kriging error method with respect to user-defined variables.

	Material	Al 2024, R = 0.1	Al 2024, R = 0.5	Austenitic	Martensitic
Applied Stress	MPa	50	50	125	75
	Euler	1.5431	1.5432	1.5431	1.5431
	Variable	1.5432	1.5433	1.5450	1.5431
	Euler	1.0902	1.0902	1.0902	1.0902
	Variable	1.0902	1.0902	1.0900	1.0902
	Euler	29,519	14,996	68,331	80,597
	Variable	29,574	15,025	68,622	80,707
Iterations	Variable	356	157	52	245

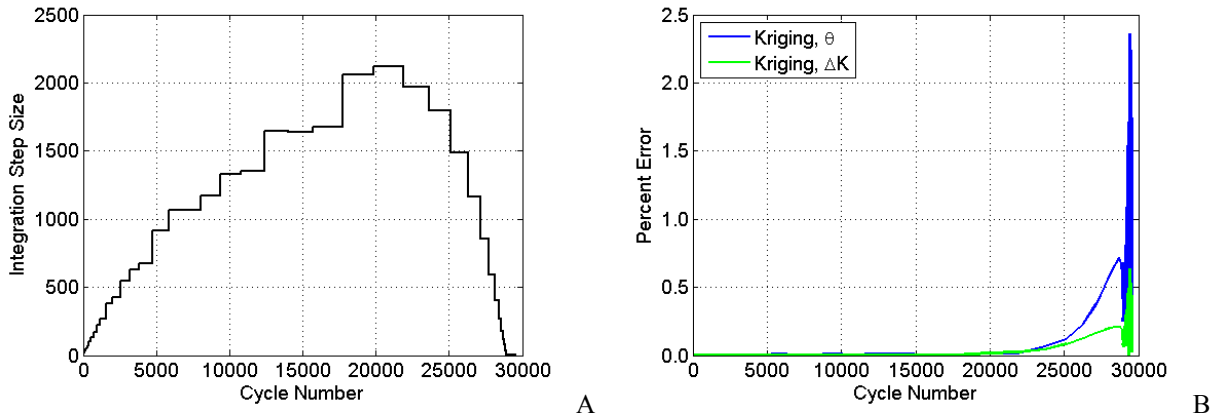


Figure 4. Integration step size (A) and percent error (B) for each cycle for aluminum 2024, R = 0.1.

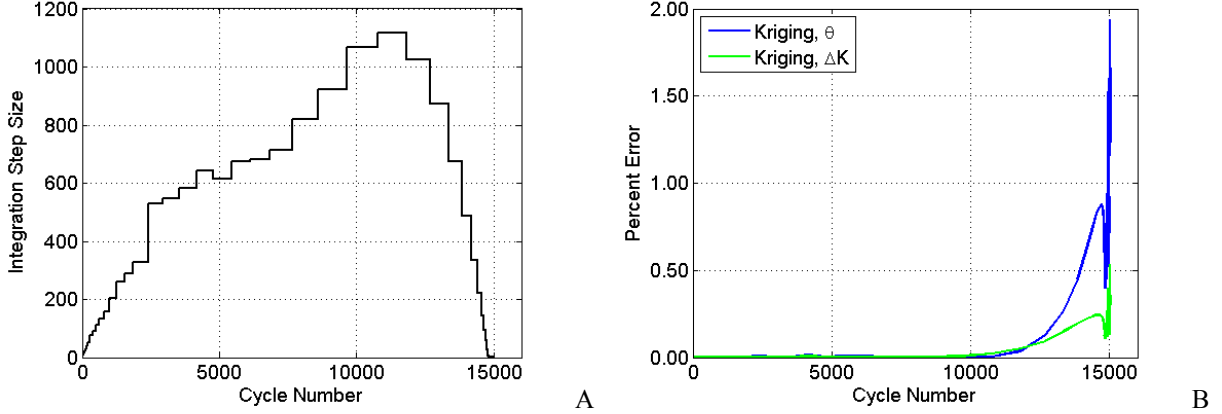


Figure 5. Integration step size (A) and percent error (B) for each cycle for aluminum 2024,  $R = 0.5$ .

## VI. Conclusions and Future Work

The ordinary differential equation which governs fatigue crack growth is not easily solved due to the fact that in general no analytical expression of the stress intensity factor as a function of crack size and crack geometry is available. Since the stress intensity factor can only be calculated at the current crack size, it is common to take a forward Euler approach to the calculation of both the magnitude and direction of crack growth for a given iteration. This limits the step size and increases the number of iterations needed to achieve sufficient accuracy.

In this paper, a kriging surrogate was used to fit the available history of the stress intensity factor and crack growth direction. The surrogate model allows one to extrapolate ahead of the current data point, enabling the use of the midpoint approximation method for the evaluation of both stress intensity factor and crack growth direction. This method produces comparable accuracy with a significantly reduced number of iterations for a range of initial crack sizes, applied stresses, materials, and crack geometries.

### Appendix A: Kriging Surrogate

Surrogate modeling is a technique of approximating a function which is expensive to evaluate with one which is less expensive. Normally the approximation is done such that the error between the original function and approximate one is minimized at a given set of points. In this paper, kriging<sup>11-13</sup> surrogate model is used to approximate a function of interest  $y(\mathbf{x})$ . As this function is expensive to evaluate, it may be approximated by a cheaper model  $\hat{y}(\mathbf{x})$  based on assumptions on the nature of  $y(\mathbf{x})$  and on the observed values of  $y(\mathbf{x})$  at a set of  $p$  data points called experimental design. More explicitly,

$$y(\mathbf{x}) = \hat{y}(\mathbf{x}) + \varepsilon(\mathbf{x}) , \quad (16)$$

where  $\mathbf{x} = [x_1, \dots, x_d]^T$  is a real  $d$ -dimensional vector of input variables and  $\varepsilon(\mathbf{x})$  represents both the error of approximation and random errors.

Kriging estimates the value of the unknown function  $y(\mathbf{x})$  as a combination of basis functions  $f_i(\mathbf{x})$  such as a polynomial basis and departures  $z(\mathbf{x})$  as

$$\hat{y}(\mathbf{x}) = \sum_{i=1}^m \beta_i f_i(\mathbf{x}) + z(\mathbf{x}) , \quad (17)$$

where  $z(\mathbf{x})$  satisfies  $z(\mathbf{x}_k) = y(\mathbf{x}_k) - \sum_{i=1}^m \beta_i f_i(\mathbf{x}_k)$  for all sample points  $(\mathbf{x}_k)$  and is assumed to be a realization of a stochastic process  $Z(\mathbf{x})$  with mean zero,

$$\text{cov}\left(Z(\mathbf{x}_i), Z(\mathbf{x}_j)\right) = \sigma^2 R(\mathbf{x}_i, \mathbf{x}_j) , \quad (18)$$

and process variance  $\sigma^2$ , and spatial covariance function given by

$$\sigma^2 = \frac{1}{p} (\mathbf{y} - \mathbf{X}\mathbf{b})^T \mathbf{R}^{-1} (\mathbf{y} - \mathbf{X}\mathbf{b}) , \quad (19)$$

where  $R(\mathbf{x}_i, \mathbf{x}_j)$  is the correlation between  $Z(\mathbf{x}_i)$  and  $Z(\mathbf{x}_j)$ ,  $\mathbf{y}$  is the value of the actual responses at the sampled points,  $\mathbf{X}$  is the Gramian design matrix constructed using the basis functions at the sample points,  $\mathbf{R}$  is the matrix of correlations  $R(\mathbf{x}_i, \mathbf{x}_j)$  among sample points, and  $\mathbf{b}$  is an approximation of the vector of coefficients  $\beta_i$  of Eq. (17). Figure 6 shows the prediction and the error estimates of kriging. It can be noticed that since the kriging model is an interpolator, the error vanishes at data points. The SURROGATES Toolbox<sup>22</sup> was used in all numerical problems.

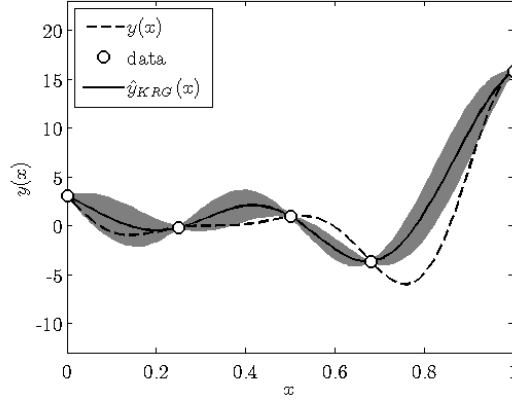


Figure 6. Kriging model  $\hat{y}_{KRG}(\mathbf{x})$  of an arbitrary set of five point and the uncertainty in gray.

## Appendix B: Extended Finite Element Method

Modeling crack growth in a traditional finite element framework is a challenging engineering task. Originally the finite element framework was modified to accommodate the discontinuities that are caused by phenomena such as cracks, inclusions and voids. The finite element framework is not well suited for modeling crack growth because the domain of interest is defined by the mesh. At each increment of crack growth, at least the domain surrounding the crack tip must be remeshed such that the updated crack geometry is accurately represented.

The extended finite element method<sup>1</sup> XFEM allows discontinuities to be represented independently of the finite element mesh. Arbitrarily oriented discontinuities can be modeled independent of the finite element mesh by enriching all elements cut by a discontinuity using enrichment functions satisfying the discontinuous behavior and additional nodal degrees of freedom. For the case of a domain containing a crack<sup>1</sup> and voids<sup>25</sup> the approximation takes the form:

$$\mathbf{u}^h(x) = V(x) \sum_{I \in \Omega} N_I(x) \left[ \mathbf{u}_I + \sum_{I \in \Omega_H} H(x) \mathbf{a}_I + \sum_{I \in \Omega_T} \sum_{\alpha=1}^4 \Phi_\alpha(x) \mathbf{b}_I^\alpha \right] \quad (20)$$

where  $N_I(x)$  are the traditional finite element shape function,  $V(x)$  is the void enrichment function,  $H(x)$  is the Heaviside enrichment function,  $\Phi_\alpha(x)$  are the crack tip enrichment functions, and  $\mathbf{u}_I$ ,  $\mathbf{a}_I$ , and  $\mathbf{b}_I$  are the classical and enriched degrees of freedom. When a node would be enriched by the Heaviside and crack tip enrichment functions, only the crack tip functions are used as is shown in Figure 7.

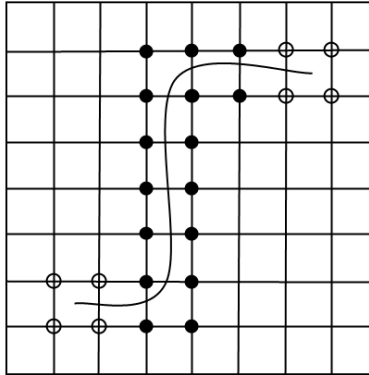


Figure 7. The location of the enriched nodes corresponding to the crack tip enrichment functions where the Heaviside enriched nodes are filled circles and crack tip enriched nodes are open circles.

To decrease the computational time for the repeated solutions, a reanalysis algorithm<sup>2</sup> is used which takes advantage of the large constant portion of the global stiffness matrix. The mixed-mode stress intensity factors for the given cracked geometry were calculated using the domain form of the interaction integrals<sup>26, 27</sup>. The direction of crack growth was calculated using the maximum circumferential stress criterion given by Eq. (6). The effective stress intensity factor was found from Eq. (5) and was used in Paris Law to calculate the magnitude of crack growth at the current iteration. Crack growth is modeled until  $\Delta K$  is greater than  $K_{IC}$ .

### References

- <sup>1</sup>Moës N., Dolbow J.E., Belytschko T., "A finite element method for crack growth without remeshing." *International Journal for Numerical Methods in Engineering*, Vol. 46, 1999, pp. 131-150.
- <sup>2</sup>Pais M., Kim N.H., Davis T.A. "Reanalysis of the extended finite element method for crack initiation and propagation." 2010, *51st AIAA/ASME/ASCE/AHS/ASC Structures, Structural Dynamics, and Materials Conference*, Orlando, FL.
- <sup>3</sup>Shi J., Chopp D.L., Lua J., Sukumar N., Belytschko T., "Abaqus implementation of extended finite element method using a level set representation for three-dimensional fatigue crack growth and life predictions." *Engineering Fracture Mechanics*, Vol. 77, 2010, pp. 2840-2863.
- <sup>4</sup>Beden S., Abdullah S., Ariffin A., "Review of Fatigue Crack Propagation Models in Metallic Components." *European Journal of Scientific Research*, Vol. 28, 2009, pp. 364-397.
- <sup>5</sup>Maligno A.R., Rajaratnam S., Leen S.B., Williams E.J., "A three-dimensional (3D) numerical study of fatigue crack growth using remeshing techniques." *Engineering Fracture Mechanics*, Vol. 77, 2010, pp. 94-111.
- <sup>6</sup>Queipo N., Haftka R., Shyy W., Goel T., Vaidyanathan R., Tucker P., "Surrogate-based analysis and optimization." *Progress in Aerospace Sciences*, Vol. 41, 2005, pp. 1-28.
- <sup>7</sup>Wang G., Shan S., "Review of metamodeling techniques in support of engineering design optimization." *Journal of Mechanical Design*, Vol. 129, 2007, pp. 370-380.
- <sup>8</sup>Forrester A.I.J., Keane A.J., "Recent advances in surrogate-based optimization." *Progress in Aerospace Sciences*, Vol. 45, 2009, pp. 50-79.
- <sup>9</sup>Simpson T.W., Toropov V., Balabanov V., Viana F.A.C. "Design and analysis of computer experiments in multidisciplinary design optimization: A review of how far we have come - or not." 2008, *12 AIAA/ISSMO Multidisciplinary Analysis and Optimization Conference*, Victoria, Canada.
- <sup>10</sup>Myers R. *Classical and Modern Regression with Applications*. Duxbury Thomson Learning: Pacific Grove, CA, 2000.

- <sup>11</sup>Kleijnen J., "Kriging metamodeling in simulation: A review." *European Journal of Operational Research*, Vol. 182, 2009, pp. 707-716.
- <sup>12</sup>Martin J., Simpson T., "Use of kriging models to approximate deterministic computer models." *AIAA Journal*, Vol. 43, 2005, pp. 853-863.
- <sup>13</sup>Stein M. *Interpolation of Spatial Data: Some Theory for Kriging*. Springer: New York, NY, 1999.
- <sup>14</sup>Cheng B., Titterton D., "Neural networks: A review from a statistical perspective." *Statistical Science*, Vol. 9, 1994, pp. 2-54.
- <sup>15</sup>Smola A., Scholkopf B., "A tutorial on support vector regression." *Statistics and Computing*, Vol. 14, 2004, pp. 199-222.
- <sup>16</sup>Chapra S., Canale R. *Numerical Methods for Engineers*. McGraw-Hill: New York, NY, 2002.
- <sup>17</sup>Paris P., Gomez M., Anderson W., "A rational analytic theory of fatigue." *The Trend in Engineering*, Vol. 13, 1961, pp. 9-14.
- <sup>18</sup>Rhee H., Salama M., "Mixed-mode stress intensity factors solutions for a warped surface flaw by three-dimensional finite element analysis." *Engineering Fracture Mechanics*, Vol. 28, 1987, pp. 203-209.
- <sup>19</sup>Tanaka K., "Fatigue crack propagation from a crack inclined to the cyclic tension axis." *Engineering Fracture Mechanics*, Vol. 6, 1974, pp. 493-507.
- <sup>20</sup>Yan X., Zhang Z., "Mixed mode criteria for the materials with different yield strengths in tension and compression." *Engineering Fracture Mechanics*, Vol. 42, 1992, pp. 109-116.
- <sup>21</sup>Sih G.C., "Strain-energy-density factor applied to mixed mode crack problems." *International Journal of Fracture*, Vol. 10, 1974, pp. 305-321.
- <sup>22</sup>Viana F.A.C. *SURROGATES Toolbox User's Guide, Version 2.1*, 2010, available at <http://sites.google.com/site/fchegury/surrogatestoolbox>.
- <sup>23</sup>Sun C.T. *Mechanics of Aircraft Structures*. John Wiley and Sons: Hoboken, NJ, 2006.
- <sup>24</sup>Mukamai Y. *Stress Intensity Factors Handbook*. Pergamon Press: New York, NY, 1987.
- <sup>25</sup>Daux C., Moës N., Dolbow J.E., Sukumar N., Belytschko T., "Arbitrary branched and intersecting cracks with the extended finite element method." *International Journal for Numerical Methods in Engineering*, Vol. 48, 2000, pp. 1741-1760.
- <sup>26</sup>Shih C., Asaro R., "Elastic-plastic analysis of crack on bimaterial interface: Part I - small scale yielding." *Journal of Applied Mechancis*, Vol. 55, 1988, pp. 299-316.
- <sup>27</sup>Yau J., Wang S., Corten H., "A mixed-mode crack analysis of isotropic solids using conservation laws of elasticity." *Journal of Applied Mechancis*, Vol. 47, 1980, pp. 335-341.